

Test of Cosmic Spatial Isotropy for Polarized Electrons Using a Rotatable Torsion Balance

Li-Shing Hou, Wei-Tou Ni, and Yu-Chu M. Li

Center for Gravitation and Cosmology, Department of Physics, Tsing Hua University, Hsinchu, Taiwan 30055, Republic of China
(Received 20 June 2000; revised manuscript received 20 February 2003; published 21 May 2003)

To test the cosmic spatial isotropy, we use a rotatable torsion balance carrying a transversely spin-polarized ferrimagnetic Dy_6Fe_{23} mass. With a rotation period of 1 h, the period of anisotropy signal is reduced from one sidereal day by about 24 times, and hence the $1/f$ noise is reduced. Our present experimental results constrain the cosmic anisotropy Hamiltonian $H = C_1\sigma_1 + C_2\sigma_2 + C_3\sigma_3$ (σ_3 is in the axis of earth rotation) to $(C_1^2 + C_2^2)^{1/2} = (1.1 \pm 2.0) \times 10^{-20}$ eV and $|C_3| = (1.1 \pm 6.0) \times 10^{-19}$ eV. This improves the previous limits on $(C_1^2 + C_2^2)^{1/2}$ by 27 times.

DOI: 10.1103/PhysRevLett.90.201101

PACS numbers: 04.80.Cc, 11.30.Cp, 11.30.Er, 98.80.Es

Einstein equivalence principle (EEP) is the cornerstone of metric theories of gravity and governs the microscopic and macroscopic structures in external gravitational fields. In metric theories (including general relativity), the EEP guarantees local Lorentz invariance. However, in the spirit of Mach, the inertial and related properties should be determined by the distribution of matter in the cosmos. To test this, Hughes-Drever-type experiments have been performed over the last 40 years with increasing precision on the anomalous atomic energy level splittings of Li [1–3], Be [4–6], and Hg [7–9]. With the advent of the concept of spontaneous broken symmetry of vacuum and the discovery of the quadrupole anisotropy in cosmic microwave background radiation [10,11], the test of cosmic isotropy at the fundamental law level and the enhancement of precision of the Hughes-Drever-type experiments become even more significant.

References [1–8] are mainly Hughes-Drever-type experiments on nuclei. Phillips worked on a Hughes-Drever-type experiment on the electron using a cryogenic torsion pendulum carrying a transversely polarized magnet with superconducting shields [12]. In 1987 [13], he set a stringent upper limit of 8.5×10^{-18} eV for the energy splitting of electron spin states. In our laboratory we have used a room-temperature torsion balance with a magnetically compensated $DyFe_3$ polarized mass to improve the limit. Our cumulated results set a limit of 3×10^{-18} eV [14–16]. Berglund *et al.* [9] have used the relative frequency of Hg and Cs magnetometers to monitor the potential energy level variations due to spatial anisotropy and give an upper limit of 1.7×10^{-18} eV for the electron. For all of these experiments, the signals to be

detected have a period of one sidereal day. Table I lists the corresponding limits given by various experiments.

For the analysis of cosmic anisotropy for electrons, we use the Hamiltonian [17]

$$H = C_1\sigma_1 + C_2\sigma_2 + C_3\sigma_3 \quad (1)$$

in the celestial frame of reference. This includes the following two cases: (i) $H_{\text{cosmic}} = g\sigma \cdot \mathbf{n}$ with $C_1 = gn_1$, $C_2 = gn_2$, $C_3 = gn_3$ as considered in [14–16] (here the C 's are constants); (ii) $H_{\text{cosmic}} = g\sigma \cdot \mathbf{v}$ with $C_1 = gv_1$, $C_2 = gv_2$, $C_3 = gv_3$ as considered in [12,13,17–19]; in this case, since \mathbf{v} is largely the velocity of our solar system through the cosmic preferred frame, to a first approximation, the C 's are also constants. For convenience, we use the celestial equatorial coordinate system with the earth-rotation axis as the z axis and the direction of the spring equinox as the positive x direction (Fig. 1). The right ascension α of our laboratory is measured eastward along the celestial equator from the spring equinox (Y) to its intersection with laboratory's hour circle. Declination δ is the geographical latitude. For our laboratory, δ is $24^\circ 47' 43''$ and the longitude is $120^\circ 59' 58''$. For a suspended electron polarized body with its net spin axis pointing in a horizontal direction rotated counterclockwise from the east direction by θ , the torque from (1) is

$$\vec{\tau} = n\vec{C} \times \langle \vec{\sigma} \rangle, \quad (2)$$

where n is the number of polarized electrons and $\langle \vec{\sigma} \rangle$ is the average polarization vector. When we suspend this polarized body with a fiber, the torque on the fiber is

$$\tau_{\text{vert}} = \frac{1}{2}n\langle \vec{\sigma} \rangle [C_1(1 + \sin\delta)\cos(\alpha + \theta) - C_1(1 - \sin\delta)\cos(\alpha - \theta) + C_2(1 + \sin\delta)\sin(\alpha + \theta) - C_2(1 - \sin\delta)\sin(\alpha - \theta) - 2C_3\cos\delta\cos\theta]. \quad (3)$$

When the torsion pendulum is rotating with angular frequency ω ,

$$\theta = \omega t + \theta_0, \quad \alpha = \Omega t + \alpha_0, \quad (4)$$

with Ω the earth-rotation angular frequency, θ_0 the initial θ angle, and α_0 the initial right ascension.

The equilibrium angular position change of the fiber is τ/K with K the torque constant of the loaded fiber. In our

TABLE I. Hughes-Drever-type experiments using electron spins. $\delta E_{\perp} = 2(C_1^2 + C_2^2)^{1/2}$ and $\delta E_{\parallel} = 2|C_3|$ are the energy level splittings parallel and transverse to the earth rotation axis, respectively [23].

Reference	δE_{\perp} (10^{-18} eV)	δE_{\parallel} (10^{-18} eV)
Phillips (1987) [13]	≤ 8.5	N.A.
Wineland <i>et al.</i> (1991) [4]	≤ 550	≤ 780
Chen <i>et al.</i> (1992) [14]	≤ 7.3	N.A.
Wang <i>et al.</i> (1992) [15]	≤ 3.9	N.A.
Chang <i>et al.</i> (1995) [16]	≤ 3.0	N.A.
Berglund <i>et al.</i> (1995) [9]	≤ 1.7	N.A.
This work	≤ 0.06	≤ 1.4

experiment, we measure this angle position change to determine C_1 , C_2 , and C_3 . For C_1 and C_2 , we use the earth rotation to perform 12-sidereal-h offset subtraction, and hence the accuracy in determining them is higher. For C_3 , the determination comes only from signals with the frequency of the rotating table, and could not be observed from a nonrotating experiment. The measurement scheme will be presented in the measurement procedure following our description of various parts of the experimental setup (Fig. 2).

The polarized-body.—To obtain large net spins for increasing the possibility of detecting an anisotropy signal while still avoiding magnetic interaction, a spin-polarized body of $\text{Dy}_6\text{Fe}_{23}$ was made as in the previous experiments [20]. The $\text{Dy}_6\text{Fe}_{23}$ ingots were crushed, pressed into a cylindrical aluminum cup, and magnetized along a transverse direction. The magnetic moment of a small sample was measured as a function of temperature from 300 to 4.2 K using an rf SQUID measurement system. We compare measurement data with model calculations to conclude that there is at least 0.4 net polarized electron per atom of $\text{Dy}_6\text{Fe}_{23}$. The net ferrimagnetic magnetization was shielded by two halves of pure iron casing, a thin aluminum spacer, and a set of two fitting

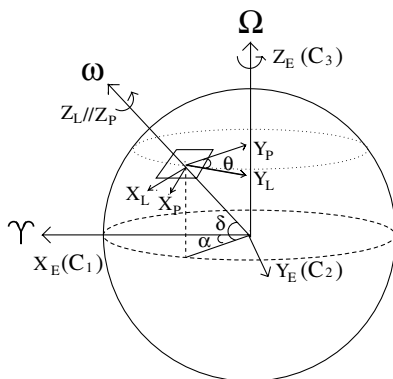


FIG. 1. The celestial equatorial frame (X_E , Y_E , Z_E), the laboratory frame (X_L , Y_L , Z_L), and the rotatable table frame (X_P , Y_P , Z_P).

201101-2

μ -metal cups. The average magnetization ($4\pi M$) after shielding is 2.57 mG.

Our $\text{Dy}_6\text{Fe}_{23}$ sample has diameter 16.0 mm, height 19.6 mm, mass 28.97 g, and number ($n|\langle\vec{\sigma}\rangle|$) of net polarized electrons 8.95×10^{22} . The magnetically shielded polarized body has a dimension of 22 mm $\phi \times$ 26 mm height with 68.3 g mass.

Torsion balance and rotatable table.—As in Fig. 2, the torsion balance is hung from the magnetic damper using a 25 μm General Electric tungsten fiber. The magnetic damper is hung from the top of the chamber housing the torsion balance using a 75 μm tungsten fiber. The period of the torsion balance is measured to be 144.34 sec with damping time 2439 sec. The moment of inertia relative to the central vertical axis of the pendulum set is 32.32 g cm^2 . Hence, the torsion constant K is 6.12×10^{-2} dyne cm/rad .

For the angle detection, we set up an optical level made of a 633 nm laser diode, a beam splitter, a mirror on the torsion balance, a 30 cm focal-length cylindrical lens, and a 3456-pixel Fairchild linear CCD with 7 μm pitch (1 pixel). A difference of 1 pixel in the CCD detection corresponds to 11.7 μrad deflection of the torsion balance and 1 nrad corresponds to 4.26×10^{-22} eV in the C 's. The torsional motion of the pendulum is damped by the D (Derivative) feedback of the coil damping system to have a damping time 292 sec without changing the equilibrium position [21].

The torsion pendulum with its housing is mounted on a rotatable table fixed to a Huber Model 440 Goniometer. The angle positioning reproducibility is better than 2 arc sec and the absolute angle deviation is less than ± 10 arc sec. The torsion balance together with the rotatable table and goniometer is mounted with four adjustable screws on the optical table inside the vacuum chamber. The four-phase stepping motor for rotating the table is

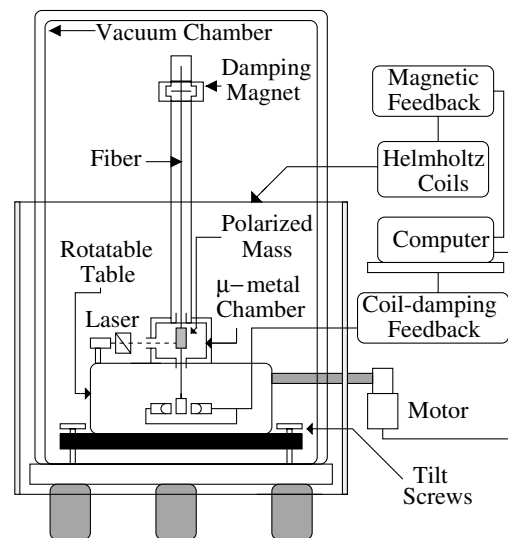


FIG. 2. Schematic experimental setup.

201101-2

outside the vacuum chamber and connected to the table by an acrylic rod. A $0.02 \mu\text{rad}$ resolution biaxial tiltmeter is attached to the table to monitor the tilt.

Magnetic field compensation and temperature control.—We use three pairs of square Helmholtz coils (1.2 m for each side) to compensate the earth magnetic field. A μ -metal chamber with attenuation factor larger than 30 is placed inside the pendulum housing to magnetically shield the polarized body. The magnetic field is measured 30 cm below the experiment chamber by a 3-axis magnetometer to make sure the region to be occupied by the μ -metal chamber and the polarized body is less than 2 mG before we set up the torsion balance. The 3-axis magnetometer signals are fed back to control the currents of three pairs of Helmholtz coils with a precision better than 0.1 mG rms.

One thermometer is attached to the middle part of the aluminum tube housing the fiber. The other four are placed outside the wall of the vacuum chamber. The chamber temperature is controlled through an air conditioner and four radiant heaters outside the chamber which are feedback controlled by these five thermometers through a personal computer. Temperature variation during a two-day data run is below 20 mK peak to peak for the thermometer on the tube.

Measurement procedure.—Each complete data run consists of four contiguous periods. Each period lasts for 12 sidereal hours (11 h 58 min 2 sec). In the first period we rotate the torsion balance clockwise or counterclockwise with 1 h period for 11 turns, and then stop the torsion balance for 58 min 2 sec to prepare for the second period. In the second period, we repeat with opposite rotation. In the third (fourth) period, we repeat with the same sense of

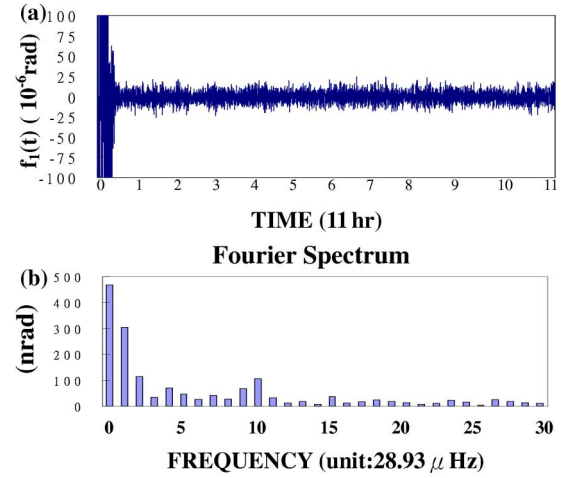


FIG. 3 (color online). (a) A typical data set for $f_1(t)$. (b) Fourier spectrum for $f_1(t)$ from $t = 1$ h to $t = 10.599$ h.

rotation as in the second (first) period. The torsion balance angular position $F(t)$ is measured. $F(t)$ is basically equal to the equilibrium position τ/K plus deviation and noise. Let T be 12 sidereal hours. Adding two data sets with the same rotating direction for F using Eqs. (3) and (4), we can eliminate C_1 and C_2 and estimate C_3 ; subtracting, we can eliminate C_3 and estimate C_1 and C_2 . For $0 \leq t \leq 12$ sidereal hours, in the case where the rotation is counterclockwise in the first period, define $F_+(t) = F(t) - F(t + 3T)$ and $F_-(t) = F(t + 2T) - F(t + T)$; in the other case, define $F_+(t) = F(t + 2T) - F(t + T)$ and $F_-(t) = F(t) - F(t + 3T)$. We form the following combinations to separate signals with different frequencies:

$$f_1(t) = \{(1 + \sin\delta)F_+(t) + (1 - \sin\delta)F_-(t)\}/(4 \sin\delta) = (n|\langle\vec{\sigma}\rangle|/K)\{C_1 \cos[(\Omega + |\omega|)t + \alpha_0 + \theta_0] + C_2 \sin[(\Omega + |\omega|)t + \alpha_0 + \theta_0]\}, \quad (5)$$

$$f_2(t) = \{(1 - \sin\delta)F_+(t) + (1 + \sin\delta)F_-(t)\}/(4 \sin\delta) = (n|\langle\vec{\sigma}\rangle|/K)\{C_1 \cos[(\Omega - |\omega|)t + \alpha_0 - \theta_0] + C_2 \sin[(\Omega - |\omega|)t + \alpha_0 - \theta_0]\}, \quad (6)$$

$$f_3(t) = \{F(t) + F(t + 3T)\}/(2 \cos\delta) = -(n|\langle\vec{\sigma}\rangle|/K)C_3 \cos(|\omega|t + \theta_0), \quad (7)$$

$$f_4(t) = \{F(t + T) + F(t + 2T)\}/(2 \cos\delta) = -(n|\langle\vec{\sigma}\rangle|/K)C_3 \cos(-|\omega|t + \theta_0). \quad (8)$$

Analysis and results.—From the fast Fourier transform (FFT) analysis of the linear-drift-reduced CCD residuals of $f_1(t)$, $f_2(t)$, $f_3(t)$, and $f_4(t)$, we obtain two estimates of C_1 , C_2 , and C_3 . Figure 3 shows a typical data set for $f_1(t)$ and its Fourier spectra. In this case, we start rotating the torsion pendulum set at 22:58:07, 16 February 1999, counterclockwise with $\theta_0 = 180$.

The feedback cycle from the CCD readout to the changing current applied to the damping coils is 80 msec. The CCD readout is, in general, not saved. Only at every 6.749 sec and at every 7.031 sec the CCD readouts

are saved (no integration or averaging); these give 5867 ($= 11 \text{ h}/6.749 \text{ sec}$) data points for $f_1(t)$ and 5632 points for $f_3(t)$ ($= 11 \text{ h}/7.031 \text{ sec}$). Because of starting transients, we discard the first hour data and use only 5120 points. For $f_1(t)$, we use the interval $t = 1$ h to $t = 10.599$ h (10 cycles for angular frequency $\Omega + |\omega|$) for Fourier analysis. At $t = 1$ h, the initial right ascension α_0 is 279.6° . From FFT, the amplitude of (C_1, C_2) is (16.4 nrad, 105.3 nrad). The average with standard deviations for C_1 and C_2 of 8 sets (16 d) of these numbers are listed in Table II. From these averages, $(C_1^2 + C_2^2)^{1/2}$ is

TABLE II. FFT amplitudes of $f_1(t)$ for the determination of C_1 and C_2 .

	C_1 (nrad)	C_2 (nrad)
1	-67.8	-56.1
2	112.3	-138.0
3	-100.6	100.5
4	-26.9	-73.7
5	32.7	-106.4
6	16.4	105.3
7	-85.4	53.8
8	-83.1	105.3
Average	-25.3 ± 26.2	-1.2 ± 36.4

determined to be $1.1(\pm 1.9) \times 10^{-20}$ eV. The reason that the 10th FFT amplitude is higher than the neighboring FFT components in Fig. 3 is due to the noise with the table-rotation frequency which falls in between the 9th and the 10th frequencies. A more detailed analysis subtracting this noise may lead to smaller uncertainties. Here we take the simple approach. Since $f_2(t)$ and $f_1(t)$ has some correlations, we use only $f_1(t)$ for data analysis.

The latter data have much less tilt effect. For clockwise rotation, these four sets of data give C_3 values, -2.1 , -2.7 , 1.5 , and $1.2 \mu\text{rad}$; for counterclockwise rotation, they give C_3 values, -0.4 , -1.8 , 1.3 , and $1.0 \mu\text{rad}$; the average with standard deviation is $(-0.25 \pm 0.61) \mu\text{rad}$. From this, C_3 is determined to be $(1.1 \pm 2.6) \times 10^{-19}$ eV.

Systematic errors.—The magnetic, temperature, and humidity responses are measured to be 257 nrad/mG, 83.5 nrad/mK, and 55 μrad per percent humidity change. The humidity is controlled to better than 0.01%. The FFT amplitudes for magnetic field, temperature, and humidity at $C_1(C_2)$ signal frequency are less than 0.3 μG , 70 μK , and $(1.5 \times 10^{-4})\%$; those at C_3 signals frequency are 0.6 μG , 140 μK , and $(2 \times 10^{-4})\%$. Maximum changes multiplied by the responses give maximum systematic errors listed in Table III.

The tilt response is measured to be 25 nrad/ μrad at 1 h rotation frequency. At other frequencies, the response is less. Two-day tilt variations are less than 40 nrad. After subtraction, the tilt effect in (C_1, C_2) measurements are less than 1 nrad. For the latter 8 d data of $f_3(t)$ and $f_4(t)$, the tilt is less than 50 μrad . The systematic error contribution in C_3 is less than 1250 nrad. Large parts of these systematic errors could be statistical and are already included in Table II. Other sources of systematic errors are also listed in Table III.

Our constraint on the Lorentz and *CPT* violation parameters \tilde{b}_\perp^e and \tilde{b}_\parallel^e of Bluhm and Kostelecky [22] is $\tilde{b}_\perp^e [= (C_1^2 + C_2^2)^{1/2}] \leq 3.1 \times 10^{-29}$ GeV and $\tilde{b}_\parallel^e (= C_3) \leq 7.1 \times 10^{-28}$ GeV.

We thank S.-s. Pan, W.-S. Tse, and H.-C. Yeh for generous help and the National Science Council for support.

TABLE III. Systematic error budget.

Sources	$(C_1^2 + C_2^2)^{1/2}$ (nrad)	C_3 (nrad)
Optical	4.3	4.8
CCD readout	3.5	3.5
Gravity noise	≤ 1	≤ 1
Timing	1.2	1.2
Tilt	1	1250
Magnetic	1	257
Temperature	5.8	12
Humidity	8.8	11
Total	12	1275

- [1] V.W. Hughes *et al.*, Phys. Rev. Lett. **4**, 342 (1960).
- [2] R.W.P. Drever, Philos. Mag. **6**, 683 (1962).
- [3] J.E. Ellena *et al.*, IEEE Trans. Instrum. Meas. **IM-36**, 175 (1987).
- [4] D.J. Wineland *et al.*, Phys. Rev. A **5**, 821 (1972).
- [5] J.D. Prestage *et al.*, Phys. Rev. Lett. **54**, 2387 (1985).
- [6] D.J. Wineland *et al.*, Phys. Rev. Lett. **67**, 1735 (1991).
- [7] S.K. Lamoreaux *et al.*, Phys. Rev. A **39**, 1082 (1989).
- [8] B.J. Venema *et al.*, Phys. Rev. Lett. **68**, 135 (1992).
- [9] C.J. Berglund *et al.*, Phys. Rev. Lett. **75**, 1879 (1995).
- [10] G.F. Smoot *et al.*, Astrophys. J. **396**, L1 (1992).
- [11] C.M. Gutiérrez *et al.*, Astrophys. J. **529**, 47 (2000).
- [12] P.R. Phillips, Phys. Rev. **139**, B491 (1965); P.R. Phillips and D. Woolum, Nuovo Cimento B **64**, 28 (1969).
- [13] P.R. Phillips, Phys. Rev. Lett. **59**, 1784 (1987).
- [14] S.-C. Chen *et al.*, *Proceedings of the Sixth Marcel Grossmann Meeting on General Relativity*, edited by H. Sato and T. Nakamura (World Scientific, Singapore, 1992), p. 1625.
- [15] S.-L. Wang *et al.*, Mod. Phys. Lett. A **8**, 3715 (1993).
- [16] F.-L. Chang *et al.*, in *Proceedings of the International Workshop on Gravitation and Cosmology* (Tsing Hua University, Hsinchu, 1995), pp. 21–29.
- [17] L.-S. Hou and W.-T. Ni, in *Proceedings of the International Workshop on Gravitation and Astrophysics, Tokyo, 1997*, edited by K. Kuroda (ICRR, Tokyo, 1998), p. 143.
- [18] L. Stodolsky, Phys. Rev. Lett. **34**, 110 (1975).
- [19] H. Nielson *et al.*, Nucl. Phys. **B211**, 269 (1983).
- [20] W.-T. Ni, in *Proceedings of the 4th Marcel Grossmann Meeting*, edited by R. Ruffini (Elsevier Science Publishers, Amsterdam, 1986), p. 1335; R.C. Ritter *et al.*, Phys. Rev. D **42**, 977 (1990); T.C.P. Chui and W.-T. Ni, Phys. Rev. Lett. **71**, 3247 (1993).
- [21] P.G. Nelson, Ph.D. thesis, University of California at Irvine, 1989.
- [22] R. Bluhm and V.A. Kostelecky, Phys. Rev. Lett. **84**, 1381 (2000); R. Bluhm *et al.*, Phys. Rev. Lett. **79**, 1432 (1997).
- [23] In the Web page <http://www.npl.washington.edu/eotwash/>, the recent results of Eöt wash spin-polarized experiment was announced with $\delta E_\perp \leq 0.12 \times 10^{-18}$ eV and $\delta E_\parallel \leq 0.44 \times 10^{-18}$ eV.